(45) Olabisi, O.; Robeson, L.; Shaw, M. *Polymer–Polymer Miscibility*; Academic: New York, 1979.
(46) Olabibi, O. *Macromolecules* **1975**, *8*, 316.
(47) Nishi, T.; Kwei, T. K. *Polymer* **1975**, *16*, 285.
(48) Shiomi, T.; Kohno, K.; Yoneda, K.; Tomita, T.; Miya, M.; Imai, K. *Macromolecules* **1985**, *18*, 414. Robard, A. Ph.D. Thesis, McGill University, 1979.
(49) Panayiotou, C.; Vera, J. H. *Fluid Phase Equil.* **1980**, *5*, 55. Panayiotou, C.; Vera, J. H. *Polym. J. (Tokyo)* **1982**, *14*, 681.
(50) Panayiotou, C.; Vera, J. H. *Can. J. Chem. Eng.* **1981**, *59*, 501.

Static and Dynamic Solution Properties of Poly(1,4-benzamide) in Dimethylacetamide with 3% (g/mL) LiCl

Qicong Ying† and Benjamin Chu*†‡

Department of Chemistry and Department of Materials Science and Engineering, State University of New York at Stony Brook, Long Island, New York, 11794-3400.
Received August 20, 1986

ABSTRACT: Laser light scattering was used to determine static and dynamic solution properties of five poly(1,4-benzamide) (PBA) samples in dimethylacetamide (DMAC) with 3% (g/mL) LiCl. The results show $\bar{D}^{\circ}_z = 1.24 \times 10^{-3} M_w^{-0.89}$ cm^2/s with M_w expressed in units of grams per mole and a persistence length ρ of 75 ± 3 nm. As the α_D (=0.89) value and the persistence length for PBA in DMAC with 3% (g/mL) LiCl are greater than those for poly(1,4-phenyleneterephthalamide) (PPTA) in concentrated sulfuric acid, PBA in DMAC/LiCl has stiffer chains than PPTA in concentrated sulfuric acid. Concentration and angular dependence of mean line widths as well as molecular weight distributions derived by using different methods of data analysis are presented.

Introduction

Dynamic light scattering in combination with static light scattering intensity measurements has been used successfully to determine both the static and dynamic properties of wormlike macromolecules in solution, such as poly(1,4-phenyleneterephthalamide) (PPTA) in concentrated sulfuric acid.[1-3] Poly(1,4-benzamide) (PBA) is another important aromatic polyamide polymer material that yields high-thermal-stability, high-modulus, and high-tensile-strength fibers from solution spinning of anisotropic dopes. PPTA and PBA have similar chemical chain structure, the only difference being the incorporation into the chain of all amide groups in the "head to tail" order for PBA and in the alternating order for PPTA. Thus, the rigidity of the PBA molecular chain greatly exceeds that of PPTA.[4] The static and dynamic solution properties of these two polymers can also be expected to be somewhat different. We have published static and dynamic light scattering characterization of PPTA in 96 wt % sulfuric acid.[2,3] The present work reports recent experimental results on static and dynamic solution properties of PBA in dimethylacetamide (DMAC) with 3% (g/mL) LiCl.

Experimental Section

1. Materials. Five different molecular weight poly(1,4-benzamide) samples were kindly provided by Professor J. Wang of the Shanghai Institute of Resins in Shanghai, China.

The solvent mixture was prepared by dissolving 3% (g/mL) LiCl, which was dried at 450 °C for 3 h, in *N,N*-dimethylacetamide (DMAC) (certified reagent ACS, Fisher Scientific Co.) and kept in a drybox before use.

Solutions at different concentrations were prepared by dilution. The stock solution was made by dissolving 0.13 g of PBA in 10 mL of filtered DMAC/LiCl solvent mixture. The middle portion of each centrifuged solution (after 2 h of centrifugation at 1 × 10^4 gravity) was transferred to a screw-capped (with Teflon packing inside) 16-mm-o.d. light scattering cell and stored in a drybox except during light scattering experiments. All measurements were completed within a few days after preparation of solution, but for sample 4 (see Table I) light scattering measurements were performed periodically over about a 1-mo. period in order to check the solution stability.

The condition for centrifugation was further tested by making light scattering measurements at upper and lower portions of a PBA solution after 6 h of centrifugation at 3 × 10^4 gravity. The agreement signified that PBA was not fractionated by centrifugation, yet our procedure was sufficient to eliminate most of the dust particles in solution.

2. Methods of Measurement. The refractive index n and the refractive index increment (dn/dc) of the DMAC/LiCl solvent mixture were determined at 30 °C by using a Brice-Phoenix differential refractometer. For the measurement of n of the solvent mixture, we used chloroform (n = 1.4446 at λ_0 = 546 nm, 25 °C) as a reference standard. At 30 °C and λ_0 = 514.5 nm, the values of n and $(\partial n/\partial C)_T$ for the solvent mixture are 1.4491 and 0.3426 mL/g, respectively.

The viscosity η_0 of the DMAC/LiCl solvent mixture was determined at 30 °C by using a Ubbelohde viscometer with cyclohexane as a reference standard

$$\eta_0/d = Ft - (B/t) \quad (1)$$

where d is the density, F is an instrument constant, and B is related to the kinetic energy term. When the flow time t is long enough (usually $t > 120$ s), the B/t term in comparison with Ft is negligibly small. At 30 °C the values of η_0 and d for the solvent mixture are 1.354 cP and 0.9596 (g/mL), respectively. The DMAC/LiCl (3% g/mL) solvent showed no absorption peak in the wavelength range between 600 and 400 nm.

The light scattering apparatus has been described elsewhere.[6] We used a Lexel Model 95 argon ion laser operating, nominally, at ~250 mW. All light scattering measurements were performed by using λ_0 = 514.5 nm. Intensity measurements were accumulated automatically every 4.5° between 18° and 135° scattering angles (θ).

Correlation function measurements were made by using a 128-channel Brookhaven Model BI-2030 digital correlator. Only those time correlation function measurements whose base-line difference between calculated and measured values was less than 0.1% were accepted. A few low-angle (18°–24°) data that showed a base-line difference of around 0.2% were also analyzed. Correlation function data were accumulated every 6° between θ = 18° and 60° and every 15° between 60° and 120°. The light

* Author to whom correspondence should be addressed. Send to Chemistry Department address.
† Department of Chemistry.
‡ Department of Materials Science and Engineering.

0024-9297/87/2220-0871$01.50/0

Table I
Static and Dynamic Properties of PBA in DMAC + 3% (g/mL) LiCl

sample	$10^{-4}M_w$	$10^{-3}A_2$, (cm^3·mol)/g^2	R_g,[a] nm	R_h,[a] nm	ρ, nm	δ	δ_0
1	5.17	1.63	32	18	75 ● 3	0.40	0.90
4	4.41				75 ± 3	0.41	0.90
5	2.88				75 ± 3	0.51	0.90
3	22.9[b]	0.59	90	66		(0.22)	
2	5.52	0.31	36		75 ± 3	0.40	0.90

[a] Estimated precision ±10%. [b] This may not be a true molecular weight of sample 3; association could be a cause for this high value.

scattering spectrometer was calibrated by using benzene and NBS-705 polystyrene in cyclohexane.

3. Methods of Data Analysis. Static Properties. For wormlike chains, the weight-average molecular weight M_w, the second virial coefficient A_2, the z-average root-mean-square radius of gyration $\langle R_g^2\rangle_z^{1/2}$, the molecular anisotropy δ, and the persistence length ρ are determined by analysis of the vertical and horizontal components (ΔR_{vv} and ΔR_{vh}) of the excess Rayleigh ratio with vertically polarized incident light using the same approach as described in our recent publications[1,2]

$$\lim_{K\to 0}(HC/\Delta R_{vv})^{1/2} = (HC/\Delta R_{vv})^{1/2}\{1 + (A_2M_w)C/[1 + (4/5)\delta^2] + ...\} \quad (2)$$

$$\lim_{K\to 0}(HC/\Delta R_{hv}) = (HC/\Delta R_{hv})_0 + \mathcal{O}(C^2) \quad (3)$$

where $(HC/\Delta R_{vv})_0 = \lim_{K\to 0}(HC/\Delta R_{vv})$ and $((HC/\Delta R_{hv})_0 = \lim_{K\to 0}(HC/\Delta R_{hv})$. The optical constant H is equal to $(4\pi n^2)(dn/dC)^2/(N_A\lambda_0^4)$, and the magnitude of the momentum transfer vector K is equal to $(4\pi n/\lambda_0)\sin(\theta/2)$.

Experimentally, by treating measurements of ΔR_{vv} and ΔR_{hv} as a function of K and C, we get

$$M_w: \quad (HC/\Delta R_{vv})_0 = 1/M_{app} = 1/[M_w(1 + (4/5)\delta^2)] \quad (4)$$

$$\langle R_g\rangle: \quad \lim_{C\to 0}(HC/\Delta R_{vv}) = (1/M_{app})[1 + (\langle R_g^2\rangle_{app}K^2)/3 + ...] \quad (5)$$

$$A_2: \quad \lim_{K\to 0}(HC/\Delta R_{vv})^{-1} = (1 + (4/5)\delta^2)M_w - 2A_2M_w^2C + \mathcal{O}(C^2) \quad (6)$$

with

$$(\Delta R_{vh}/\Delta R_{vv})_0 = [3\delta^2/(5 + 4\delta^2)] \quad (7)$$

$$\langle R_g^2\rangle_z = \{[1 + (4/5)\delta^2]/[1 - (4/5)\delta + (4/7)\delta^2]\}\langle R_g^2\rangle_{app} \quad (8)$$

The persistence length was determined by the same approach as in our previous work.[7] The slope, $Y = (1/9)\rho[L - 3\rho - (4/5)\delta_0\rho]$, obtained by plotting $\{[\Delta R_{vv}(0)/(HCM)] - (4/3)[\Delta R_{vh}(0)/(HCM)]\}$ vs. K^2 is a function of the degree of polymerization N of the macromolecule, where $\Delta R_{vv}(0) = \lim_{C\to 0}\Delta R_{vv}$ and $\Delta R_{hv}(0) = \lim_{C\to 0}\Delta R_{hv}$. Then a plot of Y against N yields $(1/9)\rho b$ and $(1/9)(3 + (4/5)\delta_0)\rho^2$ as its slope and intercept, respectively, where the contour length $L = Nb$ with b being the length of the repeating unit. Thus, both δ and ρ can be evaluated.

Dynamic Properties. The measured intensity time correlation function in the self-beating mode has the form

$$G^{(2)}(\tau) = A(1 + \beta|g^{(1)}(\tau)|^2) \quad (9)$$

where $|g^{(1)}(\tau)|$ is the first-order normalized electric field correlation function, A is the background, and β is a spatial coherence factor usually taken as an adjustable parameter in the data-fitting procedure. The mean characteristic line width $\bar{\Gamma}$ and the second moment μ_2 are defined by

$$\bar{\Gamma} = \int_0^\infty G(\Gamma)\Gamma\, d\Gamma \quad (10)$$

$$\mu_2 = \int_0^\infty G(\Gamma)(\Gamma - \bar{\Gamma})^2\, d\Gamma \quad (11)$$

The cumulants method,[8] the multiexponential singular value decomposition (MSVD) technique,[3,9] and the CONTIN[10] method are used for data analysis of the measured net self-beating autocorrelation function ($A\beta|g^{(1)}(\tau)|^2$). The magnitudes of the mean characteristic line width $\bar{\Gamma}$ and of its variance ($\mu_2/\bar{\Gamma}^2$) obtained from those methods are compared.

At small scattering angles (with $KL \lesssim 1$), the mean characteristic line width $\bar{\Gamma}$ is related to the z-average translational diffusion coefficient $\bar{D}_z$ by

$$\lim_{K\to 0}\bar{\Gamma} = \bar{D}_zK^2 \quad (12)$$

and

$$\bar{D}_z = \bar{D}_z^0(1 + k_dC) \quad (13)$$

where the superscript zero denotes the value at infinite dilution and k_d is the diffusion second virial coefficient.

At larger scattering angles, $\bar{\Gamma}$ has the form

$$\bar{\Gamma}/K^2 = \bar{D}_z(1 + f\langle R_g^2\rangle_{app}K^2) \quad (14)$$

Thus, the term $\bar{D}_z^0$ ($=\bar{\Gamma}(0,0)/K^2$) can be evaluated from plots of $(\bar{\Gamma}(C,K)/K^2)$ vs. concentration and scattering angle, similar to the Zimm plot used in static light scattering data analysis. For polydisperse polymer samples, the z-average translational diffusion coefficient at infinite dilution $\bar{D}_z^0$ obeys the scaling relation

$$\bar{D}_z^0 = K_DM_w^{-\alpha_D} \quad (15)$$

in the absence of internal motions, and the hydrodynamic radius R_h has the form

$$R_h = k_BT/(6\pi\eta_0\bar{D}_z^0) \quad (16)$$

where k_B and η_0 are the Boltzmann constant and the solvent viscosity, respectively.

Polydispersity Analysis. The normalized electric field autocorrelation function $|g^{(1)}(\tau)|$ is related to the characteristic line-width distribution $G(\Gamma)$ according to

$$|g^{(1)}(\tau)| = \int_0^\infty G(\Gamma)\exp(-\Gamma\tau)\, d\Gamma \quad (17)$$

The quantity $G(\Gamma)\, d\Gamma$ represents the fraction of the total integrated intensity scattered by particles having characteristic line width from Γ to $\Gamma + d\Gamma$. By means of eq 15, the molecular weight distribution (MWD) can be evaluated on the basis of the approximate $G(\Gamma)$ that we retrieved using the CONTIN and MSVD methods.

Results and Discussion

1. Static Properties. Equations 4–6 can be represented by a Zimm plot. However, for wormlike macromolecules a distorted Zimm plot was often observed, as shown in parts A and B of Figure 1 for PBA samples 1 and 2, respectively. Table I lists the weight-average molecular weight M_w, the z-average radius of gyration $\langle R_g^2\rangle^{1/2}$, the second virial coefficient A_2, and the molecular anisotropy δ of five PBA samples. In order to check the stability of PBA in DMAC with 3% (g/mL) LiCl, the light scattering intensity of sample 4 at different scattering angles and concentrations was measured periodically over a period of about 1 mo. A Zimm plot of those measurements is shown in Figure 2, where the cross points were measured within 2 days after the solutions were prepared and the solid points were measured within 1 mo after solution preparation. Our results show that the intensity of light scattering measured from dilute solutions with concentrations

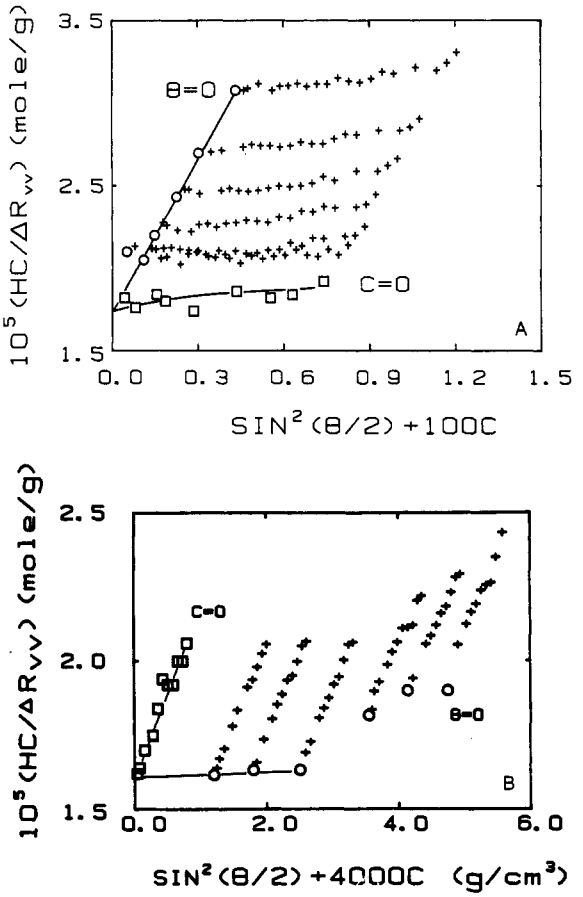

Figure 1. (A) Zimm plot for PBA sample 1 in DMAC + 3% (g/mL) LiCl. Concentrations of solution: $C1 = 5.08 \times 10^{-4}$ g/mL; $C2 = 1.09 \times 10^{-3}$ g/mL; $C3 = 1.48 \times 10^{-3}$ g/mL; $C4 = 2.24 \times 10^{-3}$ g/mL; $C5 = 3.03 \times 10^{-3}$ g/mL; $C6 = 4.32 \times 10^{-3}$ g/mL. The range of scattering angles measured 19.5°–123°. (B) Zimm plot for PBA sample 2 in DMAC + 3% (g/mL) LiCl. Concentrations of solution: $C1 = 3.01 \times 10^{-4}$ g/mL; $C2 = 4.52 \times 10^{-4}$ g/mL; $C3 = 6.28 \times 10^{-4}$ g/mL; $C4 = 8.88 \times 10^{-4}$ g/mL; $C5 = 1.04 \times 10^{-3}$ g/mL; $C6 = 1.19 \times 10^{-3}$ g/mL. The range of scattering angles measured 24°–127.5°. Hollow circles denote $\lim_{K\to 0} [HC/\Delta R_{vv}(C)]$ and hollow squares, $\lim_{C\to 0} [HC/\Delta R_{vv}(K)]$.

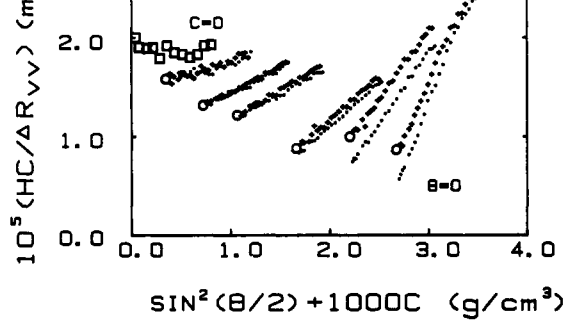

Figure 2. Zimm plot for PBA sample 4. Measurements were performed 2 days after preparation of solutions (+) and 1 mo after preparation of solutions (●). Hollow circles (○) denote $\lim_{K\to 0} [HC/\Delta R_{vv}(C)]$ and hollow squares (□), $\lim_{C\to 0} [HC/\Delta R_{vv}(K)]$.

less than 2×10^{-3} g/mL were reproducible, but for solutions with concentrations higher than 2×10^{-3} g/mL the scattered intensity increased with time after the solution preparation. This increase might be attributed to molecular association which could take place in moderate concentrations for rigid-chain macromolecules.

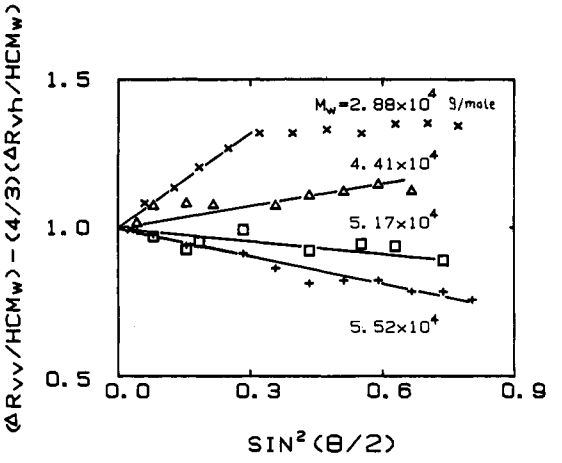

Figure 3. Plots of $[\Delta R_{vv}(0)/(HCM_w)] - (4/3)[\Delta R_{vh}(0)/(HCM_w)]$ vs. $\sin^2(\theta/2)$ for four PBA samples of different molecular weights.

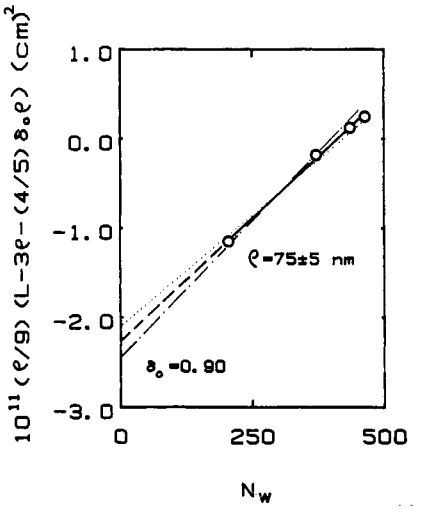

Figure 4. Plot of $Y = (1/9)\rho[L - 3 - (4/5)\delta_0\rho]$ vs. weight-average degree of polymerization N_w of PBA samples according to $Y = (1/9)\delta bN - Y_0$, where $Y_0 = (1/9)[3 + (4/5)\delta_0]\rho^2$: (—) $\rho = 75$ nm; (-·-·) $\rho = 80$ nm; (...) $\rho = 70$ nm.

Table II
Persistence Length ρ and Segment Anisotropic Factor δ_0 of PBA, Estimated from Experimental Data in Figure 4

ρ, nm	δ_0	source
75	0.90	linear least square fitting result
70	0.97	calculated from eq 8 of ref 7
76	0.84	calculated from eq 8 of ref 7
80	0.57	calculated from eq 8 of ref 7

Figure 3 shows a plot of $[\Delta R_{vv}(0)/(HCM_w)] - (4/3) \times [\Delta R_{vh}(0)/(HCM_w)]$ vs. $\sin^2(\theta/2)$ for four different molecular weight PBA samples. The slopes obtained from Figure 3 were plotted against N_w (with the subscript w denoting weight average), yielding both the persistence length $\rho = 75$ nm and the segment optical anisotropy factor $\delta_0 = 0.90$, as shown in Figure 4. By considering the possible maximum error of experimental data, we have drawn the dotted lines of $\rho = 70$ nm and $\rho = 80$ nm in Figure 4, and the value of δ_0 calculated from those intercepts which correspond with ρ values (70 nm $< \rho <$ 80 nm) are listed in Table II. A low value of δ_0 (=0.57) is not acceptable since PBA is a wormlike chain. With $\delta_0 = 0.90$, it is reasonable to consider that the persistence length of PBA, ρ, in DMAC is 75 ± 3 nm. In comparison with the results calculated from Benoit's equation (eq 8 of ref 7), Figure 5 demonstrates that $\delta_0 = 0.97$, which gave the most satisfactory fit of the experimental data to the curve $\rho =$

Table III
Comparison of Calculated Overlap Concentration C^{**} with C^+, at Which the Linear Relationship for the Concentration Dependence of $\Delta R_{vv}/(HC)$ and $\bar{\Gamma}/K^2$ Begins to Deviate

sample	$10^{-4}M_w$	L_w,[a] nm	d, nm	ρ, nm	$10^3C^+_{expt}$[b]	C^{**}_{calcd}, g/mL
1	5.17	287	0.6	75 ± 3	1.5	1.39
4	4.41	245	0.6	75 ± 3	1.6	1.44
5	2.88	160	0.6	75 ± 3	1.6	1.61
3	22.9	1.27×10^3	0.6	75 ± 3	1	0.96

[a] $L_w = (M_w/M_0)\, l_0$. $M_0 = 119$. $l_0 = 0.66$ nm.[5] [b] Estimated precision of C^+ is ±10%.

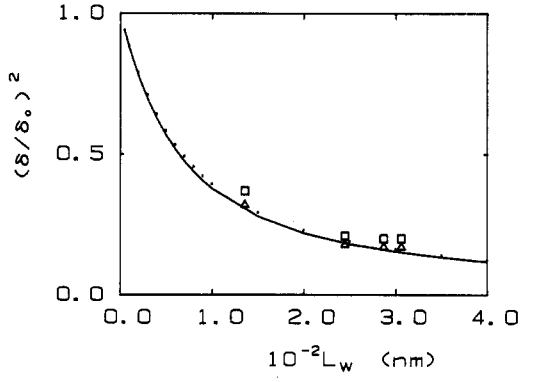

Figure 5. Plot of $(\delta/\delta_0)^2$ vs. L_w. Curves were calculated according to Benoit's equation (eq 8 of ref 2) by using different values of persistence length: (—) ρ = 75 nm; (...) ρ = 80 nm. Points are calculated from experimental data assuming different δ_0 values: (□) δ_0 = 0.90; (△) δ_0 = 0.97.

75 nm. ρ values evaluated from the two methods mentioned above are fairly consistent, with δ_0 values varying less than 10%. However, a plot of $(\delta/\delta_0)^2$ against L_w is not sensitive to the change in persistence length, as shown in Figure 5.

Arpin et al.[11] reported a persistence length of 40–60 nm for PBA in concentrated sulfuric acid, which is about 3 times higher than ρ = 17.5 nm for PPTA in concentrated sulfuric acid. A persistence length ρ = 75 ± 3 nm found in this work is 2.6 times higher than ρ = 29 nm for PPTA in concentrated sulfuric acid, as reported in our previous work.[7] Although there is disagreement for the persistence length of PPTA between the two labs, the agreement for the persistence length of PBA in two different solvents is reasonably close. There are additional persistence length values reported in the literature. For example, Prozorova et al.[13] reported ρ = 19.5 nm for PBA in DMAC with LiCl from sedimentation measurements. Schaefgen et al.[14] inferred a ρ value of 24 nm for both aromatic polyamides (PBA and PPTA). A theoretical value of ρ = 43.5 nm for aromatic polyamides was presented by Flory and Erman[15] from a rotational isomeric state calculation based on a planar and fully extended chain configuration. On the other hand, a ρ value of 105 nm for PBA in sulfuric acid was evaluated by flow birefringence measurements.[16] The 105-nm value appears quite high even if we take into account solvent quality changes between sulfuric acid and DMAC. Nevertheless, there are significant differences in the magnitude of the persistence length between our results and the literature values, but general agreement that PBA has a higher persistence length than PPTA. The higher rigidity of the PBA chain has also been verified in a theoretical deduction by Russian scientists.[12]

In crossing over from semidilute to concentrated solution regimes, several papers[2,17-19] mentioned a rather abrupt change of both static and dynamic solution properties of macromolecules. In a plot of $[\Delta R_{vv}/(HC)]$ vs. concentration at constant molecular weight of PPTA in concentrated sulfuric acid (with and without K_2SO_4),[2] a minimum value for $[\Delta R_{vv}/(HC)]_0$ occurred at concentration C_m, which can

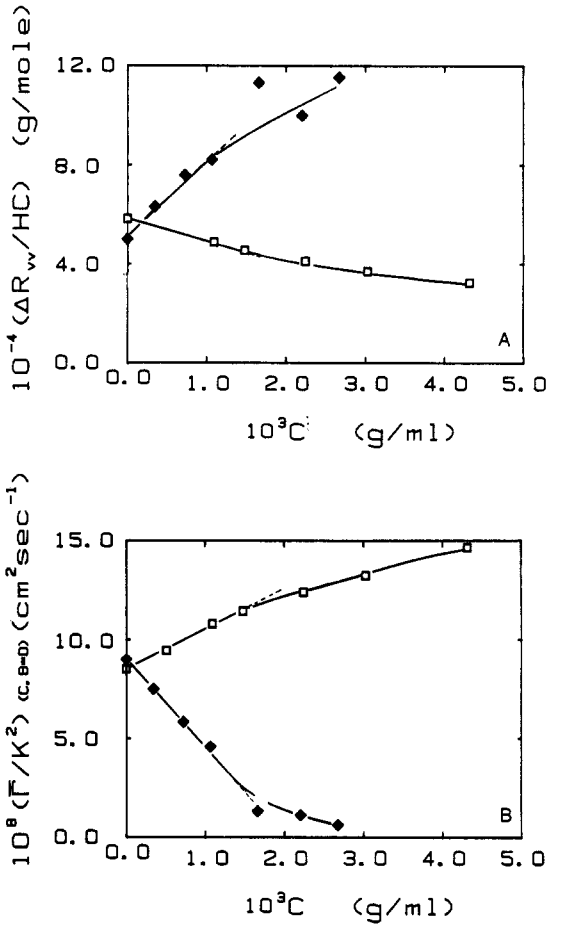

Figure 6. (A) Plots of $\Delta R_{vv}/(HC)$ vs. C for different PBA samples in DMAC + 3% (g/mL) LiCl: (□) sample 1 $M_w = 5.17 \times 10^4$; (●) sample 4 $M_w = 4.41 \times 10^4$. (B) Plots of $(\bar{\Gamma}/K^2)$ vs. C for different PBA samples as listed in A.

be regarded as the overlap threshold concentration from the semidilute to the concentrated solution regime. In our previous paper,[17] we have presented an equation for C^{**} $(=C_m)$ of wormlike macromolecules

$$C^{**} = 0.243M/(N_A d^* L^{*2}) \qquad (18)$$

where the effective length $L^* = (\rho L)^{1/2}$ and the effective diameter $d^* = (L/\rho)^{1/4}d$ can be calculated from macromolecular contour length L, diameter d, and persistence length ρ. The concentration dependence of $\Delta R_{vv}/(HC)$ and $\bar{\Gamma}/K^2$ for PBA–DMAC with 3% (g/mL) LiCl is demonstrated in parts A and B of Figure 6. However, the turnover concentration for PBA is often not as pronounced. The deviation from a linear relationship on the concentration dependence of $\Delta R_{vv}/(HC)$ and $\bar{\Gamma}/K^2$ occurs at the same concentration (C^+), which is close to the C^{**} value calculated from eq 18. It is reasonable to deduce that the value of C^+ would be less than or close to C^{**}. Values of C^{**} and C^+ are listed in Table III. Furthermore, for different PBA samples, at $C < C^+$ the value of $[\Delta R_{vv}/(HC)]$ may either increase or decrease with increasing C up to

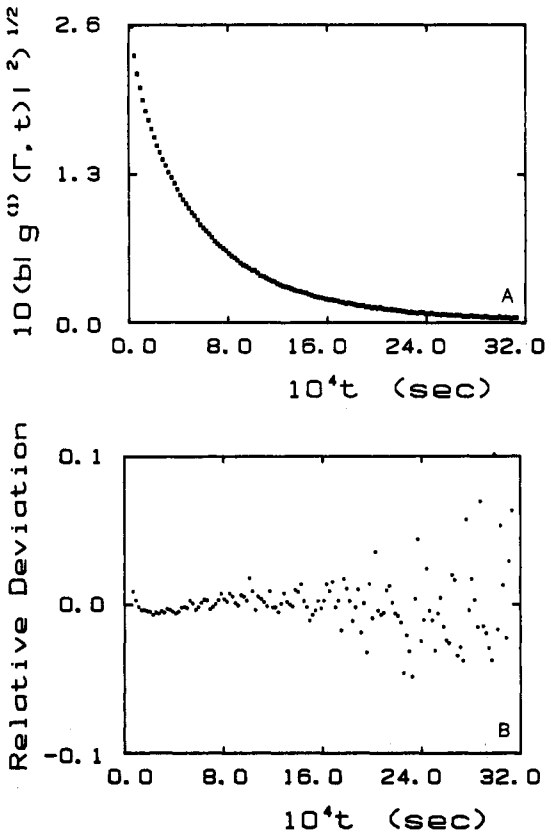

Figure 7. (A) Normalized intensity time autocorrelation function of PBA in DMAC + 3% (g/mL) LiCl at 30 °C. $C = 3.01 \times 10^{-4}$ (g/mL); $\theta = 30°$. (B) Plot of the relative deviation of the measured correlation function of A, from the calculated third-order-cumulants fit.

Table IV
Average Line Width and Variance of PBA in DMAC + 3% LiCl (g/mL) Using Different Methods of Data Analysis

method	sample	$(\Gamma)_\theta^{C,a}$ s^{-1}	$\mu/\bar{\Gamma}^2$	$10^8(\bar{\Gamma}/K^2)$, cm^2/s
third-order cumulants	1	907	0.41	8.50
	4	653	0.58	9.00
	5	1.06×10^3	0.38	11.5
	3	(211)	(0.57)	(2.00)
CONTIN	1	904	0.45	9.13
	4	726	0.43	9.81
	5	1.08×10^3	0.52	11.4
	3	(246)	(0.56)	(2.50)
MSVD	1	889	0.40	8.95
	4	704	0.71	9.54
	5	1.06×10^3	0.39	11.1
	3	(161)	(0.2)	(1.49)

[a] C denotes lowest measured concentration: sample 1, $C = 5.08 \times 10^{-4}$ g/mL; sample 4, $C = 3.45 \times 10^{-4}$ g/mL; sample 5, $C = 7.40 \times 10^{-4}$ g/mL; sample 3, $C = 3.70 \times 10^{-4}$ g/mL. Scattering angle $\theta = 30°$.

$C = C^+$ (Figure 6A), and the $(\bar{\Gamma}/K^2)$ value, in the opposite way, decreases or increases with C up to C^+ (Figure 6b); at $C = C^+$ the slope shows an apparent change.

2. Dynamic Properties. Parts A and B of Figure 7 are examples of the measured time autocorrelation function and the relative deviation of the measured correlation function of Figure 7A from a third-order-cumulants fit, respectively. The magnitude of the mean characteristic line width $\bar{\Gamma}$ and of its variance calculated from the third-order-cumulants method, the MSVD technique, and the CONTIN method are summarized in Table IV. The

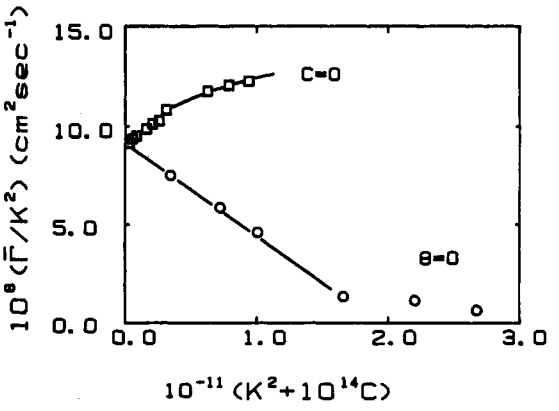

Figure 8. Plot of $(\bar{\Gamma}/K^2)$ vs. $(K^2 + 10^{14}C)$ for PBA sample 4 in DMAC + 3% (g/mL) LiCl at 30 °C.

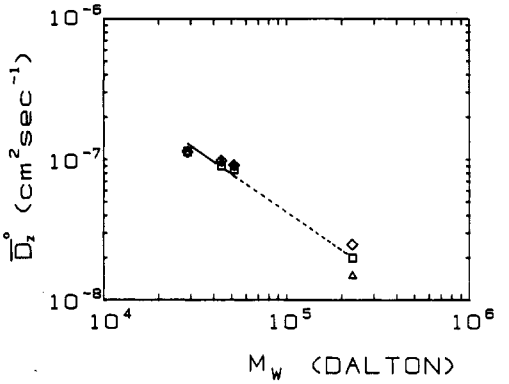

Figure 9. log–log plots of $\bar{D}_z^0$ vs. M_w at 30 °C, where $\bar{D}_z^0$ denotes the z-average translational diffusion coefficient at infinite dilution analyzed by using different methods of data analysis: (□) third-order-cumulants methods; (◇) CONTIN method; (△) MSVD method. M_w is the weight-average molecular weight.

$\bar{\Gamma}$ values obtained from those three different methods are in reasonable agreement (within 1%–8%), except for those for sample 3 which show very high molecular weight and poor fitting results by all three methods of data analysis. Association might be a cause for the abnormally high molecular weight for sample 3. At $\theta = 30°$, the value of KL_w (=11.6) is much greater than one. Thus, internal motions should be considered. Figure 8 shows a plot of $(\bar{\Gamma}/K^2)$ vs. K^2 and C for sample 4 from a third-order-cumulants fit. From the intercept $\bar{D}_z^0$ is obtained. A least-squares fitting of log $\bar{D}_z^0$ (by three independent fitting methods) vs. log M_w for four PBA samples, as shown in Figure 9, yields

$$\bar{D}_z^0 = 1.24 \times 10^{-3} M_w^{-0.89} \quad (19)$$

with $\bar{D}_z^0$ and M_w expressed in units of squared centimeters per second and grams per mole, respectively. The $(\bar{\Gamma}/K^2)_0$ values obtained by using the three independent fitting methods agree within 7%, 9%, and 4% for samples 1, 4, and 5, respectively, but ~34% for sample 3 as shown in Figure 9 and Table IV. Thus, eq 19 represents a relatively rough estimate of the scaling relation with fairly large uncertainties in both the exponent (0.89) and the amplitude factor. From the relation $\alpha_\eta = 3\alpha_D - 1$, $\alpha_\eta = 1.67$. Papkov and co-workers[12] have reported an α_η value of 1.85 for PBA in DMAC + 3% LiCl at 20 °C. Schaefgen[14] found two distinct regions: below $M_w = 1.2 \times 10^4$ $\alpha_\eta = 1.7$ and above $M_w = 1.2 \times 10^4$ $\alpha_\eta = 1.08$ for PBA in concentrated sulfuric acid. Arpin and Strazielle[11] pointed out that according to their experimental data $\alpha_\eta = 1.5$ for PBA in concentrated sulfuric acid ($4 \times 10^3 < M < 1.6 \times 10^4$) and α decreases with increasing molecular weight. As the

Table V
Average Molecular Weight and Polydispersity of MWD of PBA Using Different Methods of Data Analysis

method	sample	$10^{-4}M_n$	$10^{-4}M_w$	$10^{-4}M_z$	M_w/M_n	M_z/M_w
CONTIN	4	2.63	4.77	11.8	1.82	2.47
	5	1.81	3.00	6.69	1.66	2.23
MSVD	4	2.30	3.84	10.8	1.67	2.80
	5	2.20	3.28	8.67	1.49	2.64

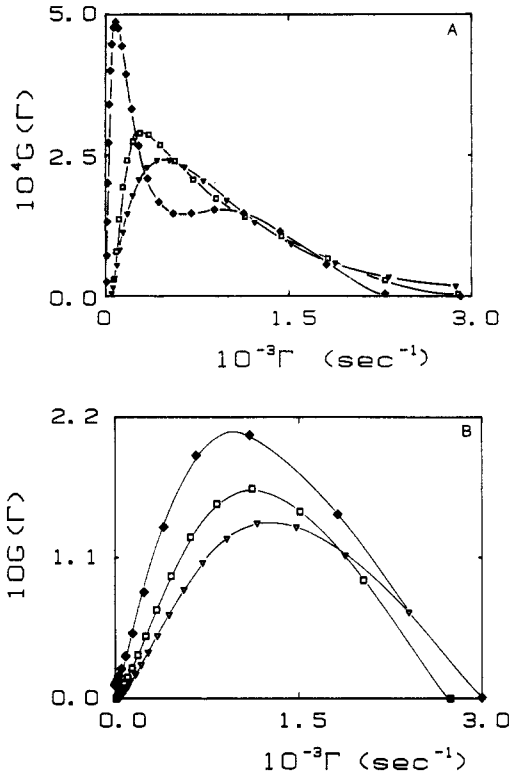

Figure 10. (A) Characteristic line-width distribution of PBA samples with different molecular weights based on the CONTIN method: (□) sample 1; (◆) sample 4; (▽) sample 5. $G(\Gamma)$ is represented by a continuous distribution curve. (B) Characteristic line-width distribution of PBA samples with different molecular weights based on the MSVD technique: (□) sample 1; (◆) sample 4; (▽) sample 5. $G(\Gamma)$ is represented by a discrete distribution curve.

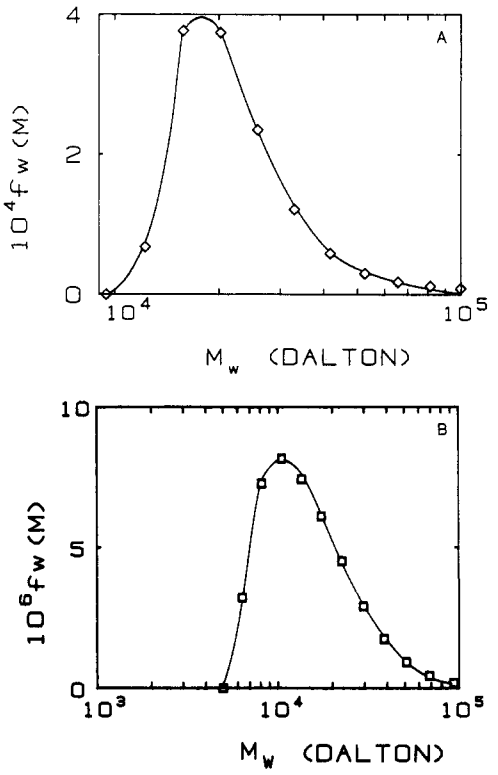

Figure 11. Molecular weight distributions of PBA samples 4 and 5 based on the CONTIN method. (A) Molecular weight distribution of PBA sample 4 ($M_z/M_w/M_n$ 4.49/1.81/1). (B) Molecular weight distribution of PBA sample 5 ($M_z/M_w/M_n$ 6.13/2.58/1).

published intrinsic viscosity data were quite scattered, there is no a priori reason to accept the literature value as reliable. In comparison with PPTA, the high α_η and ρ values show PBA to have wormlike chain behavior.

3. Molecular Weight Distribution. The characteristic line-width distribution, $G(\Gamma)$, of PBA samples 1, 4, and 5 retrieved by using CONTIN and MSVD methods are shown in parts A and B of Figure 10, respectively. The continuous $G(\Gamma)$ curve as obtained by the CONTIN method appeared to distribute more uniformly with less emphasis at the low-frequency limit than the discrete $G(\Gamma)$ curve based on the MSVD method. For sample 4, the CONTIN method showed two peaks in the $G(\Gamma)$ distribution curve (Figure 10A), but the data retrieved by using the MSVD technique showed only one narrow peak with a long high frequency tail distribution (Figure 10B). The molecular weight distributions (MWD) of samples 4 and 5 were evaluated on the basis of $G(\Gamma)$ curves by using CONTIN and MSVD methods together with eq 19. Parts A and B of Figure 11 show the molecular weight distribution of samples 4 and 5 by the CONTIN method. A comparison of MWDs for sample 5 analyzed by both CONTIN and MSVD is shown in Figure 12. The molecular weight and polydispersity index calculated from MWD of samples 4 and 5 are summarized in Table V.

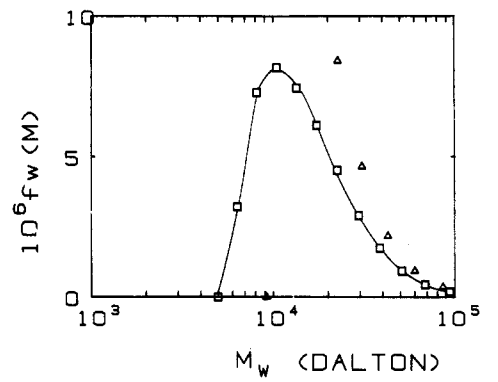

Figure 12. Comparison of the molecular weight distribution analyzed by using the CONTIN method (□) and the MSVD technique (△) for PBA sample 5.

The MWD analyzed by using the CONTIN method exhibited higher M_w/M_n but lower M_z/M_w values when compared with those obtained by the MSVD method. M_w values analyzed by the CONTIN method are closer to the results measured by the static method (for sample 5 within 1%; for sample 4 within 7.5%) than those analyzed by the MSVD technique. Both M_n and M_w values of sample 5 with monopeak MWD obtained by the CONTIN method are lower than those obtained by the MSVD technique. The discrepancy suggests that the high-frequency tail of $G(\Gamma)$ based on the MSVD technique is perhaps underestimated. On the other hand, the low-frequency tail of $G(\Gamma)$

based on the MSVD technique is overestimated. In the molecular weight range 2.89×10^4–$\sim 4.4 \times 10^4$, the polydispersity, M_w/M_n, is around 1.7–1.8 according to the MWD based on the CONTIN method. Our CONTIN results agree with the GPC analysis on similar PBA samples in DMAC with 4 wt % LiCl, as reported by Schaefgen.[14] Both methods (light scattering and GPC) showed M_w/M_n is around 1.7–1.8 for PBA samples of $M_w > 1 \times 10^4$.

In summary, we found a larger persistence length, a higher α_D (thus higher α_η) value, and a higher molecular anisotropy value for PBA in DMAC with 3% (g/mL) LiCl than those of PPTA in concentrated sulfuric acid. Thus, the PBA chain is more rigid than the PPTA chain. The experimentally measured C^+ values are close to C^{**} (eq 18) values for all PBA samples studied. The measured self-beating net autocorrelation functions have been analyzed by using the cumulants technique and the MSVD and CONTIN methods. MWD results from different methods of data analysis are compared. For unimodel distributions both MSVD and CONTIN methods are reliable. For bimodal distributions, the CONTIN method is more reliable.

With recent advances in photon correlation spectroscopy and Laplace inversion methods, laser light scattering characterization of polymer molecular weight distributions is within reach as a routine technique for hard to characterize speciality polymers.

Acknowledgment. We gratefully acknowledge support of this research by the National Science Foundation (DMR Polymers Program 8314193 and INT8211992).

Registry No. PBA (SRU), 24991-08-0; PBA (homopolymer), 25136-77-0.

References and Notes

(1) Wong, C.-P.; Ohnuma, H.; Berry, G. C. *J. Polym. Sci., Polym. Symp.* **1978**, *No. 65*, 173.
(2) Ying, Q.; Chu, B.; Qian, R.; Bao, J.; Zhang, J.; Xu, C. *Polymer* **1985**, *26*, 1401.
(3) Chu, B.; Ying, Q.; Wu, C.; Ford, J. R.; Dhadwal, H. S. *Polymer* **1985**, *26*, 1480.
(4) Tsvetkov, V. N.; Shtennikova, I. N. *Macromolecules* **1978**, *11*, 306.
(5) Alfonso, G. C.; Bianchi, E.; Ciferri, A.; Russo, S.; Salaris, F.; Valenti, B. *J. Polym. Sci., Polym. Symp.* **1978**, *No. 65*, 213.
(6) DiNapoli, A.; Chu, B.; Cha, C. *Macromolecules* **1982**, *15*, 1174.
(7) Ying, Q.; Chu, B. *Makromol. Chem., Rapid Commun.* **1984**, *5*, 785–791.
(8) Koppel, D. E. *J. Chem. Phys.* **1972**, *57*, 4814.
(9) Ford, J. R.; Chu, B. In *Proceedings of the 5th International Conference on Photon Correlation Techniques in Fluid Mechanics*; Springer-Verlag: New York, 1983; pp 303–314.
(10) Provencher, S. W. *Comput. Phys. Commun.* **1982**, *27*, 213–227, 229–242.
(11) Arpin, M.; Strazielle, C. *Polymer* **1977**, *18*, 591.
(12) Papkov, S. P.; Kulchikhin, V. G.; Kalmykova, V. D.; Malkin, A. Ya. *J. Polym. Sci., Polym. Phys. Ed.* **1974**, *12*, 1753.
(13) Prozorova, G. E.; Pavlov, A. V.; Yovleva, M. N.; Antipova, R. N.; Kalmykova, V. D.; Papkov, S. P. *Vysokomol. Soedn., Ser. B* **1976**, *18*, 111.
(14) Schaefgen, J. R.; Foldi, V. S.; Logullo, F. M.; Good, V. H.; Gulrich, L. W.; Killian, F. L. *Polym. Prepr. (Am. Chem. Soc., Div. Polym. Chem.)* **1976**, *17*, 69.
(15) Erman, B.; Flory, P. J. *Macromolecules* **1980**, *13*, 484.
(16) Tsvetkov, V. N.; Kudriavtsev, G. I. *Dokl. Akad. Nauk. SSSR* **1975**, *224–225*, 1126.
(17) Ying, Q.; Chu, B. *Macromolecules*, in press.
(18) Leger, L.; Hervet, H.; Rondelez, R. *Macromolecules* **1981**, *14*, 1732.
(19) Zero, K. M.; Pecora, R. *Macromolecules* **1982**, *15*, 87.

Dilute and Concentrated Solution Properties of Zigzag Polymers Comprising Long Rodlike Segments with Freely Rotating Joints

Shaul M. Aharoni

Engineered Materials Sector Laboratories, Allied Corporation, Morristown, New Jersey 07960. *Received May 29, 1986*

ABSTRACT: Nine fully aromatic, highly regular "zigzag" polyamides and poly(ester amides) were prepared, each consisting of identical virtual bonds with freely rotating joints joining them along the chain. The length l_0 of the virtual bonds ranged from 10.6 Å up to 44.7 Å. In dilute solutions the behavior of the zigzag polymers is dictated by their freely rotating joints, with their rodlike segments acting as long virtual bonds in freely rotating random coils. The poly(ester amides) behave as highly draining coils, while the polyamides are nondraining. The size of the zigzag polymer coils is clearly dependent on l_0. Their Kuhn segment length A approximates three virtual bonds. In concentrated solutions the solution behavior is dominated by M_w and C and to a lesser extent by l_0. The effect of the virtual bond length is especially noticeable when the viscosity is normalized to remove the effects of differences in chain length. At very high concentrations the zigzag polymers do not form lyotropic liquid crystals despite the fact that their rodlike segments are of sufficient length to form anisotropic solutions. In the bulk, the zigzag polymers do not form thermotropic liquid crystals. A chemically similar rodlike poly(ester amide) forms both lyotropic and thermotropic liquid crystals. The density of the semicrystalline zigzag polyamides and, especially, the amorphous zigzag poly(ester amides) indicates that the polymeric chains are packed just as well as in other polymers with much shorter l_0.

Introduction

Solution properties of polymers are generally treated in terms of three models: the flexible Gaussian coil, the rigid rod, and the semiflexible molecule whose flexibility is due to a gradual accumulation of the effects of small thermal vibrations of valence angles, bonds, etc.[1] Such semiflexible chains are commonly treated by the persistent coil model of Kratky and Porod[2] or by the helical wormlike chain model of Yamakawa.[3–5] Another group of semiflexible polymers is the one whose flexibility is a consequence of relatively easy transitions between several rotational isomers. Such polymers will be the focus of the present study. The chains of each of the rotational isomeric semiflexible polymers in this work are represented by a sequence of identical rodlike segments, each characterized by a virtual bond of length l_0 and a diameter d. The rodlike segments are joined together by essentially freely rotating joints. The polymers in this study can be visualized, hence, as

0024-9297/87/2220-0877$01.50/0